Photo-Cross-Linked Self-Assembled Poly(ethylene oxide)-Based Hydrogels Containing Hybrid Junctions with Dynamic and Permanent Cross-Links

Erwan Nicol, Taco Nicolaï, Jingwen Zhao, Tetsuharu Narita

HAL Id: hal-01945126

https://hal.sorbonne-universite.fr/hal-01945126v1

Submitted on 5 Dec 2018

Photo-Cross-Linked Self-Assembled Poly(Ethylene Oxide) Based Hydrogels Containing Hybrid Junctions with Dynamic and Permanent Crosslinks

Erwan Nicol[a,*], Taco Nicolai[a], Jingwen Zhao[b], Tetsuharu Narita[b,c]

[a] IMMM – UMR CNRS 6283, Le Mans Université, avenue O. Messiaen, 72085 Le Mans cedex 9, France

[b] Laboratoire Sciences et Ingénierie de la Matière Molle, ESPCI Paris, PSL University, Sorbonne Université, CNRS, 75005 Paris, France

[c] Global Station for Soft Matter, Global Institution for Collaborative Research and Education, Hokkaido University, Sapporo, Japan

Supporting Information Placeholder

ABSTRACT: Homogeneous hydrogels were formed by self-assembly of triblock copolymers via association of small hydrophobic endblocks into micelles bridged by large poly(ethylene oxide) central blocks. A fraction of the endblocks was photo-cross-linkable and could be rapidly crosslinked covalently by in-situ UV irradiation. In this manner networks were formed with well defined chain lengths between homogeneously distributed hybrid micelles that contained both permanent and dynamically crosslinked endblocks. Linear rheology showed a single relaxation mode before in-situ irradiation intermediate between those of the individual networks. The presence of transient crosslinks decreased the percolation threshold of the network rendered permanent by irradiation and caused a strong increase of the elastic modulus at lower polymer concentrations. Large amplitude oscillation and tensile tests showed significant increase of the fracture strain caused by the dynamic crosslinks.

Hydrogels are soft materials containing a large volume fraction of water. Due to their physical properties close to those of tissues in humans, they are of great interest in the biomedical field for drug or protein delivery[1-10], tissue engineering[2, 7, 8, 11-20] or cell immobilization[1, 8, 21]. However, hydrogels usually suffer from poor mechanical properties that limit their use in applications. This is true in particular for poly(ethylene oxide) (PEO), which is one of the most commonly used synthetic polymers for biomedical applications[22]. Various strategies have been developed to address this problem[23] such as topological gels[24], interpenetrated polymer networks (IPN)[25, 26], double networks (DN)[27-29], nanocomposite gels[30, 31] or flawless networks[32, 33] with impressive improvement of toughness. However, most of these hydrogels are synthesized by free radical polymerization (FRP) or "click coupling" which limits their application if injectability or biocompatibility is needed. It also involves out of equilibrium formation of the gels leading to ill-defined networks. Polymeric hydrogels can be formed in dynamic equilibrium by exploiting the spontaneous association of triblock copolymers containing hydrophobic endblocks and a hydrophilic central block[34-36]. Transient crosslinks can subsequently be rendered covalent by introducing photo-crosslinkable units within the hydrophobic blocks[37-39].

This approach has been exploited in the past to form interpenetrated self-assembled polymer networks (IPSAN) by mixing two types of triblock copolymers that formed independent interpenetrated networks[40]. The transient crosslinks of one network were subsequently rendered covalent by in-situ UV irradiation. Even though the networks were topologically independent, physical interaction between both networks led to a shift of the percolation concentration (C_p) and to a large increase of the elastic modulus compared to simple additivity. However, no significant enhancement of the gel toughness was observed, which we attribute to the fact that the networks were independent.

Here, self-assembly of triblock copolymers is exploited in a different manner. Two types of copolymers are mixed with the same central PEO block and different relatively short hydrophobic endblocks. Crosslinks formed by one type of endblock can be rendered covalent by in-situ UV irradiation, whereas the other remains dynamic. It will be shown that the two types of endblocks are randomly mixed in hybrid micellar cores. In this manner we were able to synthesize for the first time homogeneous self-assembled hydrogels containing both dynamic and permanent crosslinks with well-defined chain lengths between the crosslinks.

The dynamic network was formed by association of poly(isobutyryloxyethyl acrylate)-*b*-poly(ethylene oxide)-*b*-poly(isobutyryloxyethyl acrylate) (PIEA$_7$-*b*-PEO$_{270}$-*b*-PIEA$_7$ called IEI$_{12K}$). The photo-cross-linkable network was formed by poly(methacryloyloxyethyl acrylate)-*b*-poly(ethylene oxide)-*b*-poly(methacryloyloxyethyl acrylate) (PMEA$_7$-*b*-PEO$_{270}$-*b*-PMEA$_7$ and PMEA$_9$-*b*-PEO$_{800}$-*b*-PMEA$_7$ called tPEO$_{12K}$ and tPEO$_{35k}$, respectively) These copolymers were synthesized following methods published elsewhere[40-43] (see Supporting Information) according to the route shown in Scheme 1. In aqueous solution IEI$_{12K}$ and tPEO self-assemble into flower-like micelles that can bridge leading to a network above C_p. The apparent molar masses (M_a) and hydrodynamic radii (R_a) of the micelles obtained from light scattering were close to the averages calculated from values obtained with individual systems (see Supporting Information). It follows that either the aggregation number (N_{agg}) of the hybrid micelles was the same as the calculated average or that hybridization had not occurred.

Scheme 1. Synthesis of PMEA-b-PEO-b-PMEA (tPEO) and PIEA-b-PEO-b-PIEA (IEI) triblock copolymers.
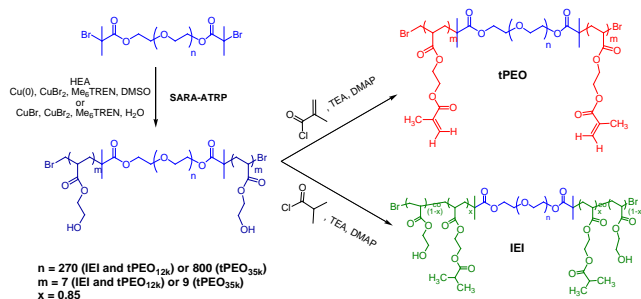
Formation of transient networks by the copolymers caused a sharp increase of the relative viscosity (η_r) with increasing concentration above C_p: $C_p \approx 15$ g/L for tPEO$_{12k}$ and IEI$_{12K}$ and $C_p \approx 8$ g/L for tPEO$_{35k}$ (Figure S5). The mechanical relaxation of transient gels formed by self-assembly of tPEO/IEI mixtures above C_p was determined by oscillatory shear measurements. The frequency dependence of the storage (G') and loss (G'') shear moduli showed a single relaxation mode that shifted to lower frequencies with increasing weight fraction of tPEO (x) in the mixtures (Figure S6). Master curves could be obtained by superimposition of results obtained at different concentrations, different chain lengths and different weight fraction using horizontal (a_x) and vertical (b_x) shift factors, see Figure 1a. This implies that the relaxation process of all systems was similar with a characteristic relaxation time that depended on the composition.

The relaxation time (τ) was defined here as the inverse of the radial frequency ($1/2\pi\nu$) at which G' crossed G''. It was intermediate between that of the individual gels and increased exponentially with x, see Figure 1b. These observations are best explained if we assume that the network was formed by bridged hybridized micelles so that the escape of PMEA was facilitated by the presence of PIEA and the escape of PIEA was slowed down by the presence of PMEA leading to single intermediate relaxation time.

The self-assembled transient hybrid gels were subsequently irradiated with UV-light in the presence of a photoinitiator, which caused covalent cross-linking of the PMEA endblocks of tPEO within the micellar cores. *In-situ* measurements during photo-cross-linking showed a very rapid increase of G' upon irradiation, see Figure 2a and Figure S7. The appearance of a frequency independent storage modulus higher than G'' at low frequencies confirmed the formation of a covalent hydrogel, see Figure 2b and Figure S8. Mixtures with relatively high concentrations of IEI$_{12K}$ still showed significant relaxation of G' at high frequencies. We suggest that this was caused by escape of PIEA blocks implying that permanently cross-linking PMEA by UV-irradiation did not trap the PIEA blocks that were present in the same hybrid cores (scheme 2).
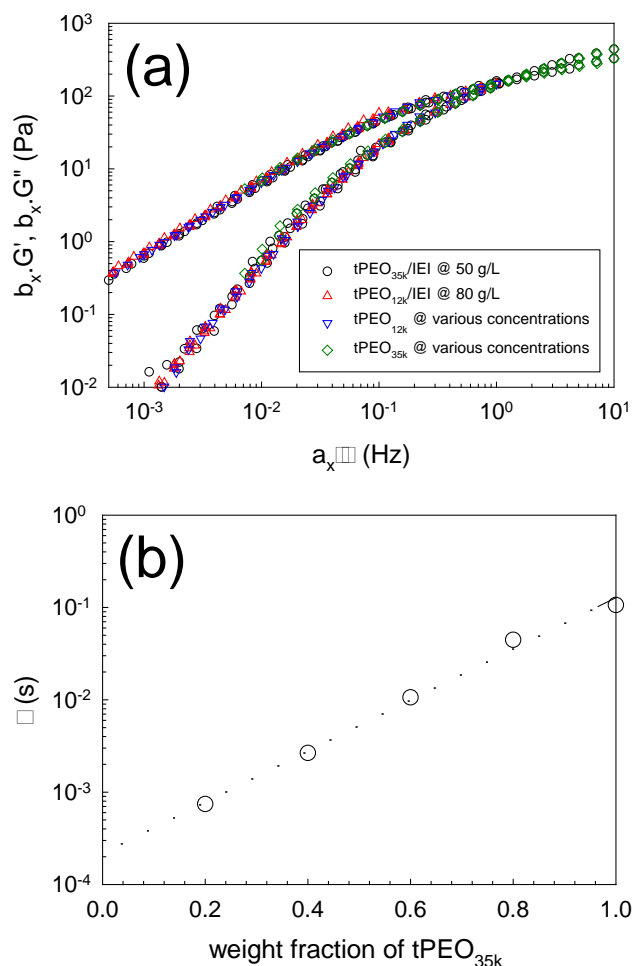

Figure 1. **(a)** Master curve obtained by superimposition the relaxation spectra of pure tPEO solutions and tPEO/IEI$_{12K}$ mixtures (reference curve: tPEO$_{35k}$ at $C = 50$ g/L and $T = 20$ °C). **(b)** Evolution of the relaxation time with the weight fraction of tPEO$_{35k}$ in tPEO$_{35k}$/IEI$_{12K}$ mixtures at $C_{tot} = 50$ g/L and $T = 20$ °C.

Scheme 2. Schematic representation of hybrid dynamic/covalent self-assembled photo-cross-linked hydrogels.
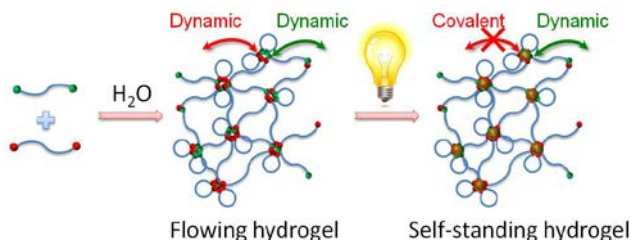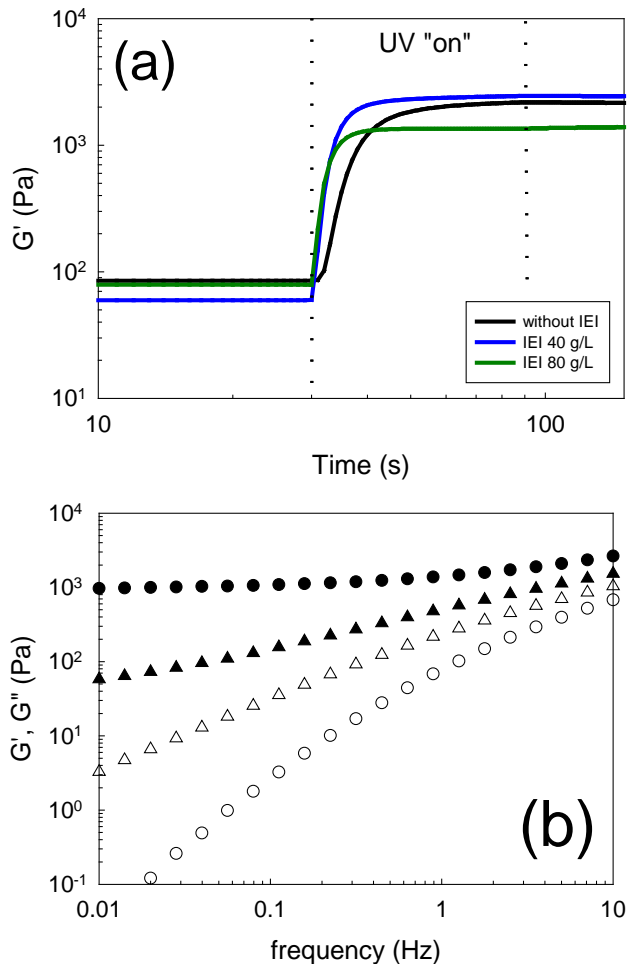
Figure 2. (a) Evolution of the elastic modulus (G') during the photo-cross-linking step of tPEO$_{35k}$/IEI$_{12K}$ hybrid hydrogels at constant tPEO$_{35K}$ concentration $C_{tPEO} = 40$ g/L and various IEI$_{12K}$ concentration indicated in the Figure. ($\gamma = 2$ %, $f = 1$ Hz). (b) Frequency dependence of the storage (G', circles) and loss (G'', triangles) moduli before (open symbols) and after UV-irradiation (filled symbols) of tPEO$_{35k}$/IEI$_{12K}$ (40 g/L-80 g/L) mixture.

At low frequencies the dynamic IEI$_{12K}$ network has completely relaxed and G' at 0.01 Hz is equal to the elastic modulus (G_0) of the covalent network. Assuming rubber elasticity and affine deformation, the ideal elastic modulus is obtained if all tPEO chains are elastically active: $G_0 = CRT/M_n$. The calculated moduli are 0.58, 1.15 and 2.31 kPa for tPEO$_{35k}$ hydrogels, at $C = 10$, 20 and 40 g/L, respectively. As shown in Figure 3, close to C_p individual tPEO hydrogels formed imperfect networks in which the fraction of elastically active chains is small. Increasing the concentration increased the fraction of elastically active chains leading to a fully formed network at $C > 40$ g/L for tPEO$_{35k}$.

For tPEO concentrations above, but close to C_p, addition of IEI$_{12K}$ triblock copolymer led to an increase of G_0, see Figure 3 and Figure S9. Considering that at low frequencies IEI$_{12K}$ chains no longer contributed to the shear modulus, the increase of G_0 was caused by an increasing number of elastically active tPEO chains in the network. In the case of highly imperfect tPEO networks close C_p, the increase caused by adding IEI$_{12K}$ could be as much as two orders of magnitude (Figure S9). This

means that adding IEI$_{12K}$ improves the connectivity of the tPEO network, though G_0 did not reach the values calculated for ideal tPEO networks.

Interestingly, similar improvement of the mechanical properties could be obtained by addition of the diblock copolymer poly(isobutyryloxyethyl acrylate)-*b*-poly(ethylene oxide)$_{5k}$ (IE). IE is equivalent to the IEI$_{12K}$ triblock copolymer cut in halve and cannot bridge micelles (Figure S10). This means that the effect of IEI$_{12K}$ on the elastic modulus of the tPEO network is not caused by transient bridging of IEI$_{12K}$, but by the presence of dynamic hydrophobic blocks in the hybrid micellar cores.

As was mentioned above, light scattering measurements showed that N_{agg} of the hybrid micelles was close to the average of the individual systems. The implication is that added PIEA blocks of either IE or IEI$_{12K}$ substituted PMEA blocks of tPEO in the micellar cores. This caused an increase of the concentration of micelles containing tPEO, which in turn favored the formation of bridges instead of loops by tPEO and therefore an increase of the fraction of elastically active tPEO chains. G_0 started to decrease again at relatively high IEI$_{12K}$ concentrations, when the molar fraction of IEI$_{12K}$ in the hybrid micelles (defined as $2n_{IEI12k}/(2n_{IEI12k}+2n_{tPEO35k})$ assuming that the PIEA and PMEA blocks are homogeneously distributed in the cores of hybrid micelles) became larger than about 70 – 85 mol%, see Figure 3. This can be explained by the fact that at high IEI$_{12K}$ concentrations an increasing fraction of micelles no longer contain sufficient number of tPEO chains to participate in the permanent tPEO network.
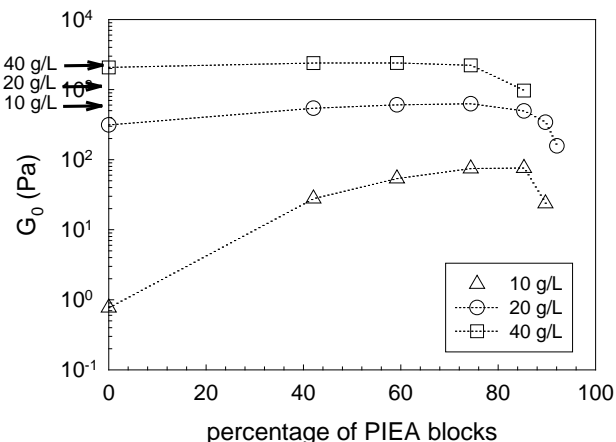

Figure 3. Evolution of the low frequency storage modulus (measured at 0.01 Hz) as a function of the molar percentage of PIEA blocks in the micelle cores for tPEO$_{35k}$/IEI$_{12k}$ hybrid hydrogels. The total concentration of block copolymer is indicated in the Figure. Dotted lines are guide to the eye. Arrows show the maximum moduli calculated assuming rubber elasticity and affine deformation.

The non-linear rheological properties of the cross-linked hydrogels were assessed using two kinds of measurements. First, G' and G'' were measured for tPEO$_{12k}$/IEI$_{12k}$ mixtures as a function of the applied strain after *in situ* photo-cross-linking at 1 Hz. Notice that the dynamic crosslinks of these mixtures were fully relaxed at this frequency. As expected, at constant copolymer concentration, substituting covalent links by dynamic ones led to a decrease of G' and an increase of the fracture strain (Figure S11). Figure 4a shows that if the amount of IEI$_{12K}$ was increased while keeping the tPEO$_{12k}$ concentration constant, not only G_0 increased as discussed above, but also the fracture strain in-

3

creased. In common covalent hydrogels, increasing the number of elastically active chains increases G_0, but decreases the fracture strain[37]. Kean et al.[44] showed that adding very dynamic cross-links in a covalent organogel improved the toughness but did not enhance G_0. Here, a synergetic effect was observed not only for the stiffness (increase of elastic modulus) but also for the non-linear properties of the hydrogels (increase of the toughness).

Uniaxial stretching experiments were used to assess the evolution of the tensile stress with increasing strain (Figure 4b-c). As expected, gels obtained from tPEO$_{35k}$ exhibited larger extensibility than those obtained from tPEO$_{12k}$ with the same elastic modulus, because the elastically active chains are longer and thus more extensible. The effect of adding IEI$_{12K}$ was to substantially increase the strain at breakage (up to 350%) without reducing the Young modulus thus corroborating the large oscillation amplitude measurements. The better resistance of hybrid hydrogels to fracture can be explained by a higher capacity to dissipate energy when mechanical strain is applied, because the dynamic network can rearrange and thereby prevent stress concentration at the vicinity of the broken permanent chains. A cyclic loading-unloading experiment (Figure S12) showed small hysteresis implying that dynamic rearrangement and the stress reduction was quite fast compared to the macroscopic loading rate[44].
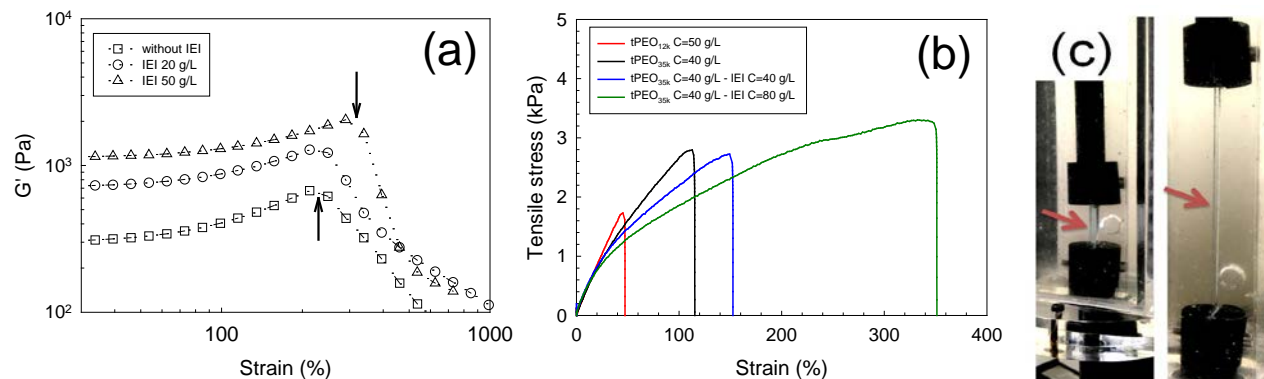

Figure 4. (**a**) Strain dependence of the elastic modulus (G') measured at $f = 1$ Hz for tPEO$_{12k}$/IEI$_{12K}$ hybrid photo-cross-linked hydrogels at constant tPEO concentration ($C = 30$ g/L) and increasing concentration of IEI$_{12K}$ as indicated in the Figure. Arrows indicate the breakage of the sample. (**b**) Tensile tests of tPEO based hydrogels after photo-cross-linking (stretch rate $v = 0.03$ s^{-1}). (**c**) Tensile test of tPEO$_{35k}$ $C = 40$ g/L – IEI$_{12K}$ $C = 80$ g/L at the beginning (left) and end (right) of the test.

To conclude, we present here a novel type of hydrogel formed by self-assembly of two types of POE-based triblock copolymers of which one is photo-cross-linkable. The novelty is that the same junction zones contain both dynamic and covalent crosslinks. Formation of hybridized micellar cores before irradiation was confirmed by the evolution of the characteristic relaxation time of a single relaxation mode with the composition of the copolymer mixtures. Photo-cross-linking of the copolymer mixtures at thermodynamic equilibrium very rapidly turned the physical (and potentially injectable) hydrogel into a self-standing covalent hydrogel formed by one of the copolymers with the other remaining dynamic. The coexistence of both dynamic and covalent crosslinks in the same junctions led to synergetic effects that enhanced the elastic modulus and the resistance of the gels to fracture. These block copolymer based hydrogels are non-cytotoxic[45] and could be interesting candidates for utilization as injectable and *in situ* photo-cross-linkable scaffolds for tissue engineering.

ASSOCIATED CONTENT

Supporting Information

Materials and methods. Structure of tPEO/IEI$_{12K}$ mixtures. Rheological properties of tPEO/IEI$_{12K}$ mixtures before photo-cross-linking. Photo-cross-linked hybrid covalent/dynamic hydrogels.

The Supporting Information is available free of charge on the ACS Publications website. brief description (PDF).

AUTHOR INFORMATION

Corresponding Author

Correspondence should be addressed to Erwan Nicol. Erwan.nicol@univ-lemans.fr. Phone: ++33.2.43.83.33.62

4

REFERENCES

(1) T. Garg, O. Singh, S. Arora and R. S. R. Murthy. Scaffold: A Novel Carrier for Cell and Drug Delivery. *Critical Reviews in Therapeutic Drug Carrier Systems* 2012, 29, 1-63.

(2) M. Goldberg, R. Langer and X. Q. Jia. Nanostructured materials for applications in drug delivery and tissue engineering. *Journal of Biomaterials Science-Polymer Edition* 2007, 18, 241-268.

(3) W. R. Gombotz and D. K. Pettit. BIODEGRADABLE POLYMERS FOR PROTEIN AND PEPTIDE DRUG-DELIVERY. *Bioconjugate Chemistry* 1995, 6, 332-351.

(4) J. Jagur-Grodzinski. Polymeric gels and hydrogels for biomedical and pharmaceutical applications. *Polymers for Advanced Technologies* 2010, 21, 27-47.

(5) B. Jeong, S. W. Kim and Y. H. Bae. Thermosensitive sol-gel reversible hydrogels. *Advanced Drug Delivery Reviews* 2002, 54, 37-51.

(6) C. C. Lin and K. S. Anseth. PEG Hydrogels for the Controlled Release of Biomolecules in Regenerative Medicine. *Pharmaceutical Research* 2009, 26, 631-643.

(7) I. Roy and M. N. Gupta. Smart polymeric materials: Emerging biochemical applications. *Chemistry & Biology* 2003, 10, 1161-1171.

(8) B. V. Slaughter, S. S. Khurshid, O. Z. Fisher, A. Khademhosseini and N. A. Peppas. Hydrogels in Regenerative Medicine. *Advanced Materials* 2009, 21, 3307-3329.

(9) M. W. Tibbitt, J. E. Dahlman and R. Langer. Emerging Frontiers in Drug Delivery. *Journal of the American Chemical Society* 2016, 138, 704-717.

(10) T. R. Hoare and D. S. Kohane. Hydrogels in drug delivery: Progress and challenges. *Polymer* 2008, 49, 1993-2007.

(11) J. L. Drury and D. J. Mooney. Hydrogels for tissue engineering: scaffold design variables and applications. *Biomaterials* 2003, 24, 4337-4351.

(12) J. Elisseeff. Injectable cartilage tissue engineering. *Expert Opinion on Biological Therapy* 2004, 4, 1849-1859.

(13) N. E. Fedorovich, J. Alblas, J. R. de Wijn, W. E. Hennink, A. J. Verbout and W. J. A. Dhert. Hydrogels as extracellular matrices for skeletal tissue engineering: state-of-the-art and novel application in organ printing. *Tissue Engineering* 2007, 13, 1905-1925.

(14) H. Geckil, F. Xu, X. H. Zhang, S. Moon and U. Demirci. Engineering hydrogels as extracellular matrix mimics. *Nanomedicine* 2010, 5, 469-484.

(15) A. S. Hoffman. Hydrogels for biomedical applications. *Advanced Drug Delivery Reviews* 2002, 54, 3-12.

(16) D. W. Hutmacher. Scaffolds in tissue engineering bone and cartilage. *Biomaterials* 2000, 21, 2529-2543.

(17) J. L. Ifkovits and J. A. Burdick. Review: Photopolymerizable and degradable biomaterials for tissue engineering applications. *Tissue Engineering* 2007, 13, 2369-2385.

(18) P. B. Malafaya, G. A. Silva and R. L. Reis. Natural-origin polymers as carriers and scaffolds for biomolecules and cell delivery in tissue engineering applications. *Advanced Drug Delivery Reviews* 2007, 59, 207-233.

(19) J. F. Mano, G. A. Silva, H. S. Azevedo, P. B. Malafaya, R. A. Sousa, S. S. Silva, L. F. Boesel, J. M. Oliveira, T. C. Santos, A. P. Marques, N. M. Neves and R. L. Reis. Natural origin biodegradable systems in tissue engineering and regenerative medicine: present status and some moving trends. *Journal of the Royal Society Interface* 2007, 4, 999-1030.

(20) M. S. Shoichet. Polymer Scaffolds for Biomaterials Applications. *Macromolecules* 2010, 43, 581-591.

(21) A. C. Jen, M. C. Wake and A. G. Mikos. Review: Hydrogels for cell immobilization. *Biotechnology and Bioengineering* 1996, 50, 357-364.

(22) K. Knop, R. Hoogenboom, D. Fischer and U. S. Schubert. Poly(ethylene glycol) in Drug Delivery: Pros and Cons as Well as Potential Alternatives. *Angewandte Chemie-International Edition* 2010, 49, 6288-6308.

(23) C. W. Peak, J. J. Wilker and G. Schmidt. A review on tough and sticky hydrogels. *Colloid and Polymer Science* 2013, 291, 2031-2047.

(24) K. Ito. Novel cross-linking concept of polymer network: Synthesis, structure, and properties of slide-ring gels with freely movable junctions. *Polymer Journal* 2007, 39, 489-499.

(25) D. Myung, D. Waters, M. Wiseman, P.-E. Duhamel, J. Noolandi, C. N. Ta and C. W. Frank. Progress in the development of interpenetrating polymer network hydrogels. *Polymers for Advanced Technologies* 2008, 19, 647-657.

(26) L. H. Sperling and V. Mishra. The current status of interpenetrating polymer networks. *Polymers for Advanced Technologies* 1996, 7, 197-208.

(27) J. P. Gong. Why are double network hydrogels so tough? *Soft Matter* 2010, 6, 2583-2590.

(28) J. P. Gong, Y. Katsuyama, T. Kurokawa and Y. Osada. Double-network hydrogels with extremely high mechanical strength. *Advanced Materials* 2003, 15, 1155-1158.

(29) Y. Tanaka, J. P. Gong and Y. Osada. Novel hydrogels with excellent mechanical performance. *Progress in Polymer Science* 2005, 30, 1-9.

(30) K. Haraguchi. Nanocomposite hydrogels. *Current Opinion in Solid State & Materials Science* 2007, 11, 47-54.

(31) K. Haraguchi and T. Takehisa. Nanocomposite hydrogels: A unique organic-inorganic network structure with extraordinary mechanical, optical, and swelling/de-swelling properties. *Advanced Materials* 2002, 14, 1120-1124.

(32) T. Matsunaga, T. Sakai, Y. Akagi, U. Chung and M. Shibayama. Structure Characterization of Tetra-PEG Gel by Small-Angle Neutron Scattering. *Macromolecules* 2009, 42, 1344-1351.

(33) T. Sakai, T. Matsunaga, Y. Yamamoto, C. Ito, R. Yoshida, S. Suzuki, N. Sasaki, M. Shibayama and U.-i. Chung. Design and Fabrication of a High-Strength Hydrogel with Ideally Homogeneous Network Structure from Tetrahedron-like Macromonomers. *Macromolecules* 2008, 41, 5379-5384.

(34) T. Nicolai, O. Colombani and C. Chassenieux. Dynamic polymeric micelles versus frozen nanoparticles formed by block copolymers. *Soft Matter* 2010, 6, 3111-3118.

(35) M. A. Winnik and A. Yekta. Associative polymers in aqueous solution. *Current Opinion in Colloid & Interface Science* 1997, 2, 424-436.

(36) C. Chassenieux and C. Tsitsilianis. Recent trends in pH/thermo-responsive self-assembling hydrogels: from polyions to peptide-based polymeric gelators. *Soft Matter* 2016, 12, 1344-1359.

(37) V. Kadam, T. Nicolai, E. Nicol and L. Benyahia. Structure and Rheology of Self-Assembled Telechelic Associative Polymers in Aqueous Solution before and after Photo-Cross-Linking. *Macromolecules* 2011, 44, 8225-8232.

(38) N. Sanabria-DeLong, A. J. Crosby and G. N. Tew. Photo-Cross-Linked PLA-PEO-PLA Hydrogels from Self-Assembled Physical Networks: Mechanical Properties and Influence of Assumed Constitutive Relationships. *Biomacromolecules* 2008, 9, 2784-2791.

(39) R. Tamate, T. Ueki, Y. Kitazawa, M. Kuzunuki, M. Watanabe, A. M. Akimoto and R. Yoshida. Photo-Dimerization Induced Dynamic Viscoelastic Changes in ABA Triblock Copolymer-Based Hydrogels for 3D Cell Culture. *Chemistry of Materials* 2016, 28, 6401-6408.

(40) A. Klymenko, T. Nicolai, L. Benyahia, C. Chassenieux, O. Colombani and E. Nicol. Multiresponsive Hydrogels Formed by Interpenetrated Self-Assembled Polymer Networks. *Macromolecules* 2014, 47, 8386-8393.

(41) V. S. Kadam, E. Nicol and C. Gaillard. Synthesis of Flower-Like Poly(Ethylene Oxide) Based Macromolecular Architectures by Photo-Cross-Linking of Block Copolymers Self-Assemblies. *Macromolecules* 2012, 45, 410-419.

(42) E. Nicol, T. Derouineau, F. Puaud and A. Zaitsev. Synthesis of double hydrophilic poly(ethylene oxide)-b-poly(2-hydroxyethyl acrylate) by single-electron transfer–living radical polymerization. *Journal of Polymer Science Part A: Polymer Chemistry* 2012, 50, 3885-3894.

(43) E. Nicol and R.-P. Nzé. Supplemental Activator and Reducing Agent Atom Transfer Radical Polymerization of 2-Hydroxyethyl Acrylate from High Molar Mass Poly(ethylene oxide) Macroinitiator in Dilute Solution. *Macromolecular Chemistry and Physics* 2015, 216, 1405-1414.

(44) Z. S. Kean, J. L. Hawk, S. Lin, X. Zhao, R. P. Sijbesma and S. L. Craig. Increasing the Maximum Achievable Strain of a Covalent Polymer Gel Through the Addition of Mechanically Invisible Cross-Links. *Advanced Materials* 2014, 26, 6013-6018.

(45) A. Klymenko, T. Nicolai, C. Chassenieux, O. Colombani and E. Nicol. Formation of porous hydrogels by self-assembly of photo-cross-linkable triblock copolymers in the presence of homopolymers. *Polymer* 2016, 106, 152-158.

SYNOPSIS TOC.

Flowing hydrogel   Self-standing hydrogel
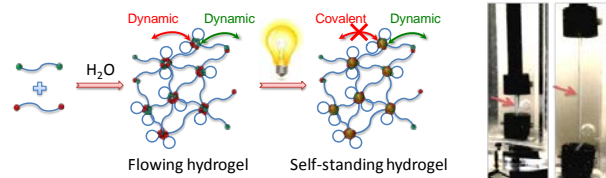
Supporting Information

Photo-Cross-Linked Self-Assembled Poly(Ethylene Oxide) Based Hydrogels Containing Hybrid Junctions with Dynamic and Permanent Crosslinks

Erwan Nicol[a,], Taco Nicolai[a], Jingwen Zhao[b], Tetsuharu Narita[b,c]*

[a] IMMM – UMR CNRS 6283, Le Mans Université, avenue O. Messiaen, 72085 Le Mans cedex 9, France

[b] Laboratoire Sciences et Ingénierie de la Matière Molle, ESPCI Paris, PSL University, Sorbonne Université, CNRS, 75005 Paris, France

[c] Global Station for Soft Matter, Global Institution for Collaborative Research and Education, Hokkaido University, Sapporo, Japan

CONTENTS

Materials and Methods

Block copolymers synthesis

Amphiphilic triblock copolymers were synthesized according to already published procedures[1-4]. Briefly, a triple hydrophilic poly(2-hydroxyethyl acrylate)-b-poly(ethylene oxide)-b-poly(2-hydroxyethyl acrylate), PHEA-b-PEO-b-PHEA, was synthesized by growing two PHEA blocks from a dibrominated PEO (Br-PEO-Br) macroinitiator using SARA-ATRP. In the case of PEO_{12k} of M_n=12 000 g/mol, the synthesis was performed in $DMSO^3$ with a molar ratio [Br-PEO-Br]/[HEA]/[Me_6TREN]/[$CuBr_2$] : 1/8/0.2/0.05. Copper wire was used as a catalyst. Prior to use the copper surface was activated with sulfuric acid. A degree of polymerization of 7 for the PHEA blocks was obtained at 90% conversion. In the case of PEO_{35k} of M_n=35 000 g/mol, the synthesis was performed in $water^4$ with a molar ratio [Br-PEO-Br]/[HEA]/[Me_6TREN]/[CuBr]/[$CuBr_2$] : 1/10/0.5/0.3/0.2. A degree of polymerization of 9 for the PHEA blocks was obtained at 90% conversion. Polymerizable methacrylate functions were then grafted onto the PHEA-blocks leading to the UV-crosslinkable hydrophobic poly(methacryloyloxyethyl acrylate) (PMEA) blocks. ^{1}H NMR analysis of both final PMEA-b-PEO-b-PMEA (tPEO) triblock copolymers indicated a quantitative functionalization of the HEA units into methacryloyloxyethyl acrylate ones. The number (M_n) and weight (M_w) average molar mass and dispersity (Đ=M_w/M_n) were determined by Size Exclusion Chromatography (SEC) in THF using light scattering and refractometric detection. M_n=1.42×10^4 g/mol, M_w=1.59×10^4 g/mol, Đ=1.1 were measured for tPEO$_{12k}$. M_n= 4.21×10^4 g/mol, M_w= 5.53×10^4 g/mol, Đ=1.3 were measured for tPEO$_{35k}$.

Poly(isobutyryloxyethyl acrylate)-b-poly(ethylene oxide)-b-poly(isobutyryloxyethyl acrylate) (PIEA-*b*-PEO-*b*-PIEA: IEI) was synthesized by esterification of PHEA-b-PEO$_{12k}$-b-PHEA with isobutyryl chloride in the presence of triethylamine and DMPA using the same procedure as that used for synthetizing PMEA-b-PEO-b-PMEA^{1,5}.^{1}H NMR analysis of the resulting IEI triblock copolymer indicated 85% of functionalization of the HEA units into isobutyryloxyethyl acrylate ones (Figure S1). The hydrophobic block was thus a statistical copolymer poly((isobutyryloxyethyl acrylate)$_{0.85}$-co-(2-hydroxyethyl acrylate)$_{0.15}$). M_n=1.42×10^4 g/mol, M_w=1.59×10^4 g/mol, Đ=1.1 were measured by multi-detection SEC.
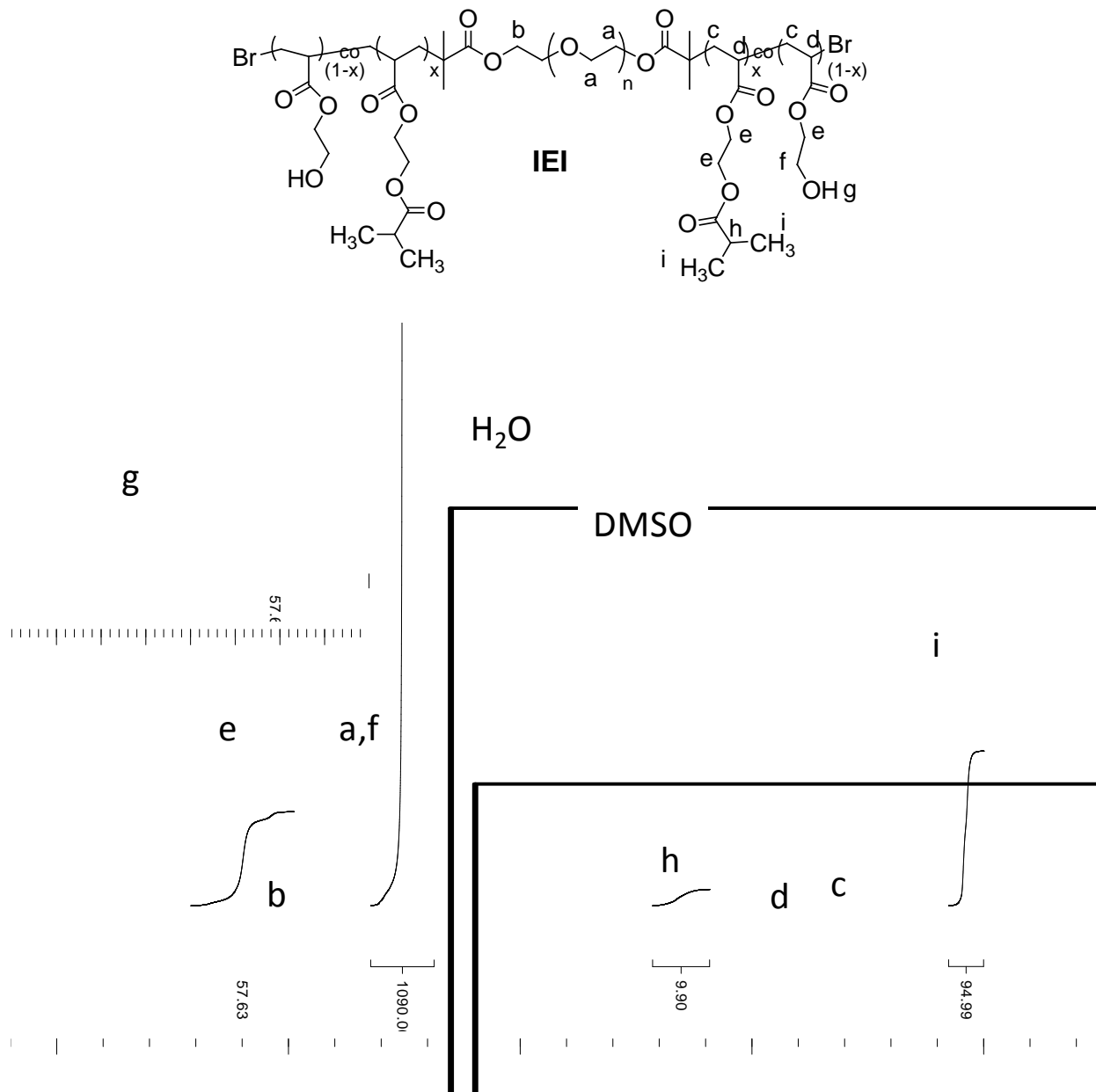
Figure S1. ^{1}H NMR of PIEA-*b*-PEO-*b*-PIEA (IEI) copolymer in DMSO-d6 (ν_0=400 MHz)

Sample preparation

Stock solutions of tPEO were prepared by dissolving the polymer powder in deionized water (MilliPore) and stored at 4 °C. For photo-cross-linking experiments a solution of 2,2-dimethoxy-2-phenylacetophenone (DMPA) photoinitiator (0.01 M) was prepared in THF. The required amount of solution of DMPA was placed on the walls of a glass vial, and THF was evaporated under a gentle flow of argon. Then, the polymer dissolved in deionized Milli-Q water was

introduced into a vial that was sealed with a rubber septum. The vial was rotated overnight on a roller stirrer. The quantity of DMPA was fixed to around 10 molecules per micelle considering the average aggregation number determined below.

Methods

Oscillatory shear measurements were done with a stress-controlled rheometer MCR-301 (Anton Paar) equipped with a cone and plate geometry (gap 0.103 mm, diameter 25 mm). For in-situ cross-linking, the samples were degassed in advance and introduced into the rheometer under gentle flow of argon. In order to prevent evaporation, the geometry was covered with silicon oil. The samples were irradiated by a UV light (Dymax Bluewave-200 lamp) at 365nm under air with an intensity 0.17 W.cm^{-1} during 60 s. The measurements were done in the linear response regime unless otherwise specified.

Static and dynamic light scattering measurements were done using a commercial static and dynamic light scattering equipment (ALV-Langen, Germany and LS-Instruments, Switzerland) operating with a vertically polarized laser with wavelength λ=632 nm. The measured scattered light intensity was corrected for that of the solvent and normalized by that of toluene. The relative excess scattering intensity (I_r) was multiplied with the Rayleigh factor of toluene and expressed in units of cm-1. The measurements were done at 20 °C using a thermostated bath over a range of scattering wave vectors (q=4.π.n.sin(θ/2)/λ), with θ the angle of observation and n the refractive index of the solvent). The electric field autocorrelation function (g1(t)) was calculated from the normalized intensity autocorrelation functions (g2(t)): g2(t)=1+g1(t)^2 and was analyzed in terms of a relaxation time distribution:

$$g_1(t) = \int A(\log \tau) \exp(- t / \tau) d \log \tau \tag{1}$$

At low polymer concentration a single relaxation mode was observed, but at higher concentrations a second slower and broader relaxation mode was observed. All correlation functions could be well-described using a log-normal distribution for the fast mode and a generalized exponential for the slow mode:

$$A(\log \tau) = k \tau^p \exp\left[- \left(\tau / \tau^*\right)^s\right] \tag{2}$$

The average relaxation rates ($\Gamma = <\tau^{-1}>$) of the single mode at low concentrations and of the fast mode at high concentrations were found to be q^2-dependent and the cooperative diffusion coefficient was calculated as

$$Dc = \Gamma . q^{-2}$$

The large deformation behavior of the gels was studied by uniaxial tensile and loading–unloading tests on an Instron 5565 tensile tester with a 10 N load cell. Samples were rectangular in shape with 5mm width, 3 mm thickness, and 20 mm length (length between clamps). We kept the samples in paraffin oil during all the tests to prevent them from drying.

Structure of tPEO/IEI mixtures

The structure of self-assemblies formed by PMEA-b-PEO-b-PMEA (tPEO) and PIEA-b-PEO-b-PIEA (IEI) triblock copolymers were studied individually and in mixtures. The apparent molar mass (M_a) and hydrodynamic radius (R_{ha}) of individual $tPEO_{12k}$ and IEI aggregates were obtained by static and dynamic light scattering as described in the materials and methods section and are shown as a function of the polymer concentration in Figure S2. As was already reported observed for similar systems in the literature[2,6] M_a and R_{ha} increased with increasing concentration due to the bridging of micelles leading to formation of larger aggregates. At high concentrations, M_a decreased because repulsive interactions dominated[6]. The number of hydrophobic blocks per micellar core (N_{agg}) could be estimated from M_a measured at 1 g/L, because at this concentration, repulsive interactions between micelles were negligible and micelles were mainly in the form of single flowers[1]. $N_{agg} \approx 60$ was found for $tPEO_{12k}$ micelles and $N_{agg} \approx 30$ for IEI_{12k} micelles. The large difference between tPEO and IEI is probably due to the lower hydrophobicity of the PIEA blocks which contained about 15% residual hydrophilic units whereas PMEA blocks did not. N_{agg} of $tPEO_{35k}$ was also approximately 30 (Figure S3).
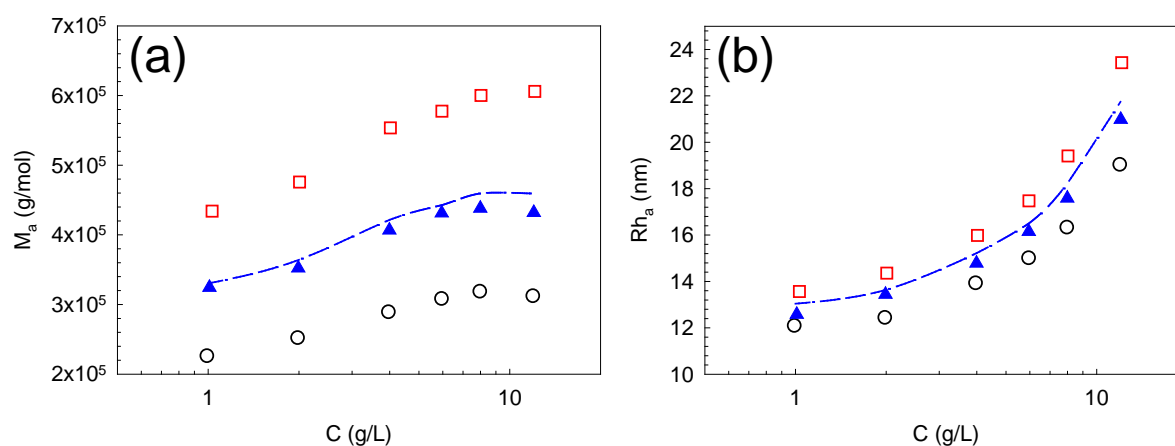
Figure S2. Concentration dependences of **(a)** the apparent molar mass (M_a) and **(b)** the apparent hydrodynamic radius (Rh_a) for the IEI aggregates (open circles), $tPEO_{12k}$ (open squares) and $tPEO_{12k}$/IEI 50/50 (%v/v) mixtures (filled triangles). Blue dashed lines represent the theoretical evolution of non-hybridizing aggregates mixture (equation (3) and (4)).
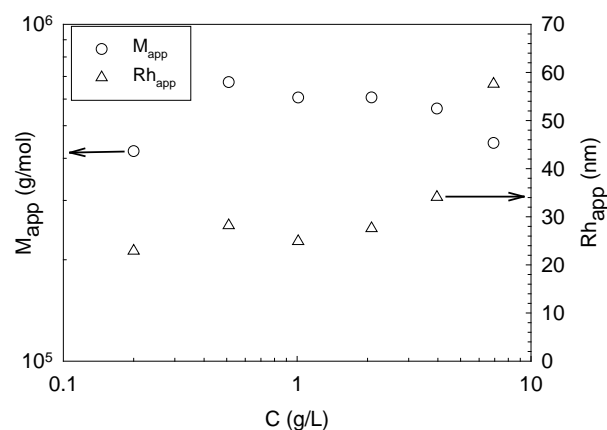

Figure S3. Concentration dependence of the apparent molar mass and apparent hydrodynamic radius of $tPEO_{35k}$ aggregates in water.

The concentration dependences of M_a and Rh_a of $tPEO_{12k}$/IEI 50/50 (vol/vol) mixtures are also shown in Figure S2. Note that all the mixtures formed homogenous transparent solutions. The same qualitative dependence was observed for the mixture and the individual systems. The

experimental data were compared with calculated values of M_a (weight-averaged) and Rh_a (z-averaged) considering no interaction between $tPEO_{12k}$ and IEI in the mixture:

$$M_a(mix) = \frac{M_a(tPEO).C(tPEO)+M_a(IEI).C(IEI)}{C(tPEO)+C(IEI)} \qquad (3)$$

$$Rh_a(mix) = \left[\frac{M_a(tPEO).C(tPEO).[Rh_a(tPEO)]^{-1}+M_a(IEI).C(IEI).[Rh_a(IEI)]^{-1}}{M_a(tPEO).C(tPEO)+M_a(IEI).C(IEI)}\right]^{-1} \qquad (4)$$

The calculated values are close to the experimental data at low polymer concentrations where the effect of interaction is small. This suggests that either hybridization did not occur or that N_{agg} of the hybrid micelles was the same as the calculated average.

Rheological properties of tPEO/IEI mixtures before photo-cross-linking

The viscosity of individual systems and mixtures was measured as function of the shear rate. All solutions exhibited Newtonian behavior over large range of shear rates, but the most viscous solutions showed shear thinning at shear rates above 10 s^{-1} (see Fig S4a and S4b).
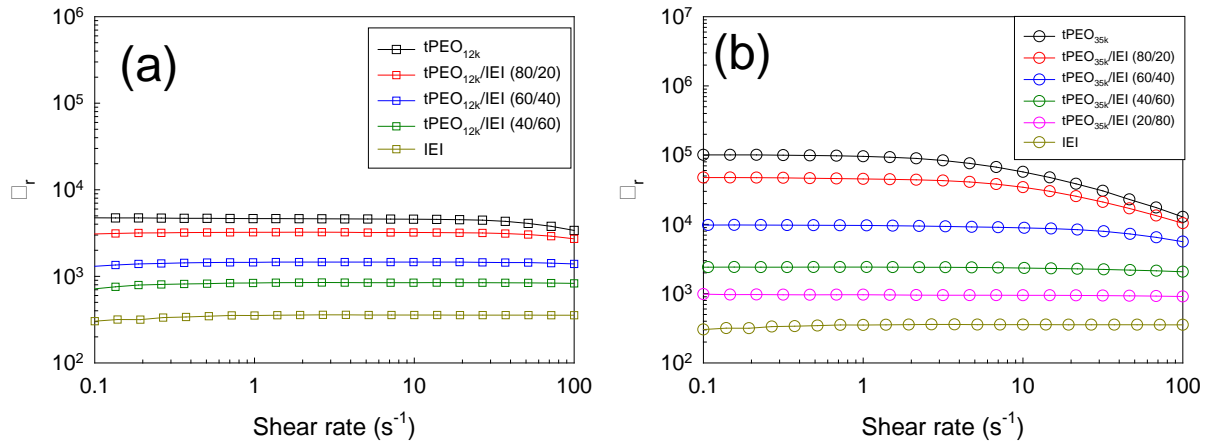

Figure S4. Shear rate dependence of the relative viscosity of **(a)** $tPEO_{12k}$/IEI hybrid hydrogels at C=50 g.L^{-1} and **(b)** $tPEO_{35k}$/IEI hybrid hydrogels at C=50 g.L^{-1}

Individual triblock copolymer solutions showed a strong increase of the relative zero-shear viscosity (η_r) with increasing concentration above a critical value (C_p) (Figure S5a). The strong increase of η_r was caused by formation of a transient network of bridged micelles and C_p

corresponds to the percolation threshold. We found $C_p \approx 15$ g/L for tPEO$_{12k}$ and IEI and $C_p \approx 8$ g/L for tPEO$_{35k}$.
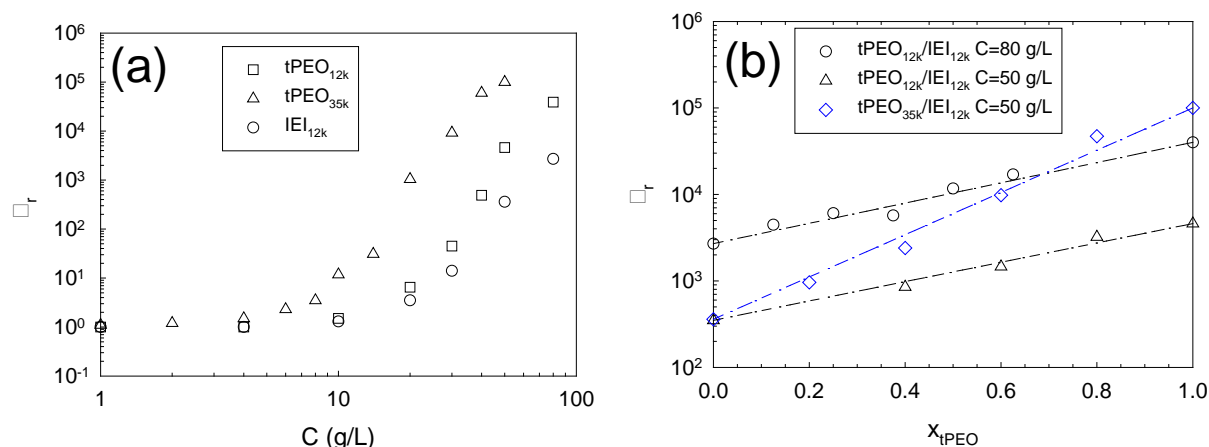

Figure S5. **(a)** Concentration dependence of the relative viscosity of IEI$_{12K}$, tPEO$_{12k}$ and tPEO$_{35k}$ at T=20 °C. **(b)** Evolution of the relative viscosity with the weight fraction of tPEO in tPEO/IEI mixtures at various concentrations. Dashed lines are fits to equation (5).

The viscosity of tPEO$_{12k}$/IEI and tPEO$_{35k}$/IEI mixtures was measured as a function of the composition C = 50 g/L. In addition, tPEO$_{12k}$/IEI mixtures were studied at C = 80 g/L. The dependence of η_r on the weight fraction of tPEO (x) in the mixtures is shown in Fig. S5b. Interestingly, for a given C, η_r had a logarithmic dependence on x:

$$\log(\eta_{r(hyb)}) = x_{tPEO}.\log(\eta_{r(tPEO)}) + x_{IEI}.\log(\eta_{r(IEI)}) \tag{5}$$

This behavior noticeably differs from that exhibited by mixtures of other types of self-assembled triblock copolymers[7,8]. In the case of hydrophobically end-capped PEO, Annable et al. [7] reported that chains with different end-cap alkyl lengths relaxed independently. This implies that the viscosity of the mixtures was governed by the polymers with the longest relaxation time, i.e. the highest viscosity. In the case of mixtures of pH-sensitive amphiphilic triblock copolyelectrolytes the viscosity was also governed by that of the most viscous copolymer as soon as it formed a percolated network [8]. In this latter case, although the evolution of the viscosity was not strictly proportional to the evolution of the mean relaxation time τ (lifetime of a hydrophobic block in a micellar core), it followed the same tendency.

The frequency dependence of the shear moduli was determined as a function of *x*. It showed a single relaxation mode that shifted to lower frequencies with increasing *x*, see Fig. S6.
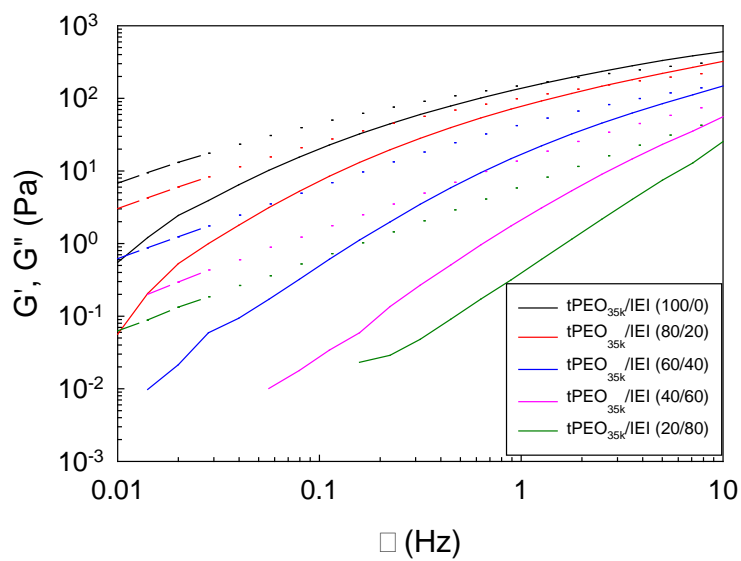

Figure S6. Frequency dependences of the storage (G') and loss (G") moduli of tPEO$_{35k}$/IEI mixtures at C$_{tot}$=50 g/L and T=20 °C.
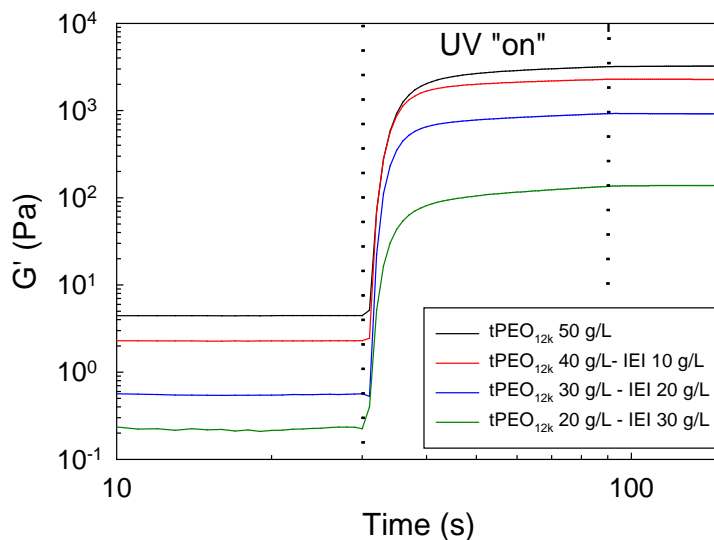
Photo-cross-linked hybrid covalent/dynamic hydrogels

Figure S7. Evolution of the elastic modulus (G') during the photo-cross-linking step of tPEO$_{12k}$/IEI hybrid hydrogels at constant polymer concentration C = 50 g/L (γ=2 %, f=1 Hz)
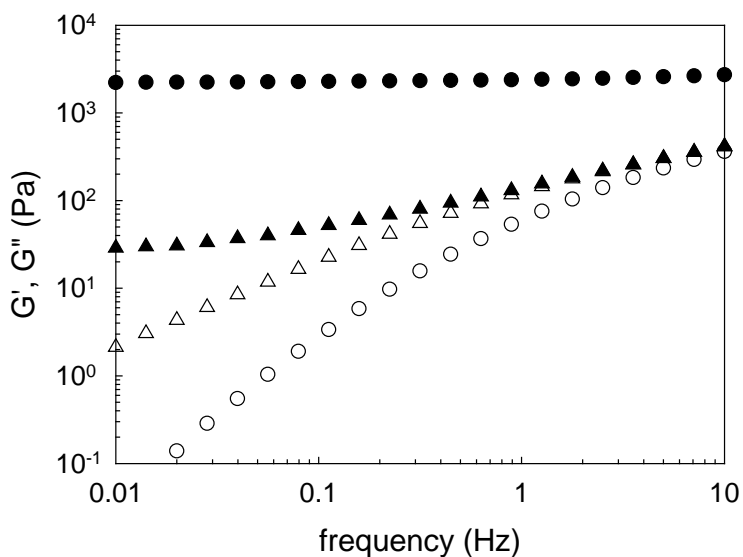

Figure S8. Frequency dependence of the storage (G', circles) and loss (G", triangles) moduli before (open symbols) and after UV-irradiation (filled symbols) of tPEO$_{35k}$/IEI (40 g/L-40 g/L) mixture
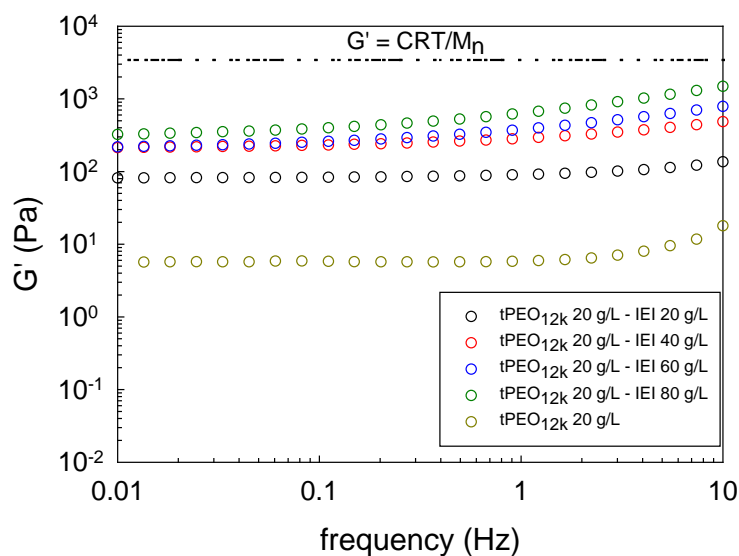
Figure S9. Frequency dependence of the storage modulus of photo-cross-linked hybrid tPEO$_{12k}$/IEI for C$_{tPEO12k}$=20 g/L and various concentration of IEI. The dashed line corresponds to the theoretical value of G' using the affine model assuming that all the tPEO$_{12k}$ chains are elastically active.
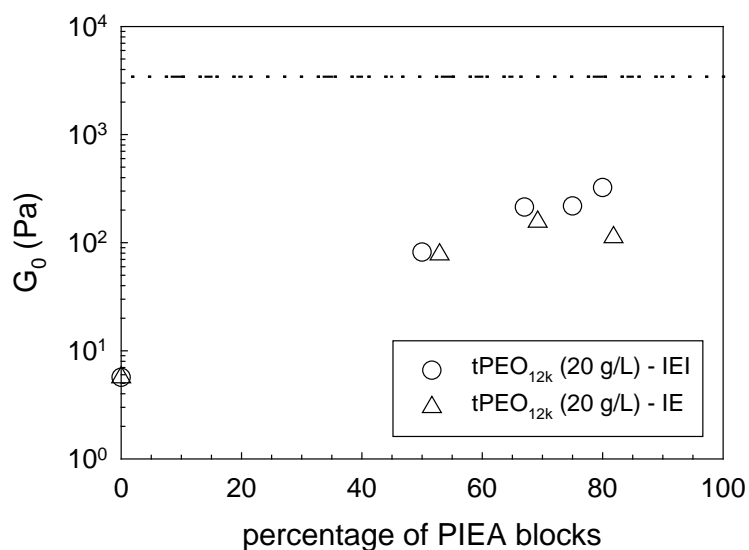

Figure S10. Evolution of the low frequency storage modulus (measured at 0.01 Hz) as a function of the molar percentage of PIEA blocks in the micelle cores for tPEO$_{12k}$ (C=20 g/L) mixed with IEI triblock copolymer (circles) or IE diblock copolymer (triangle)
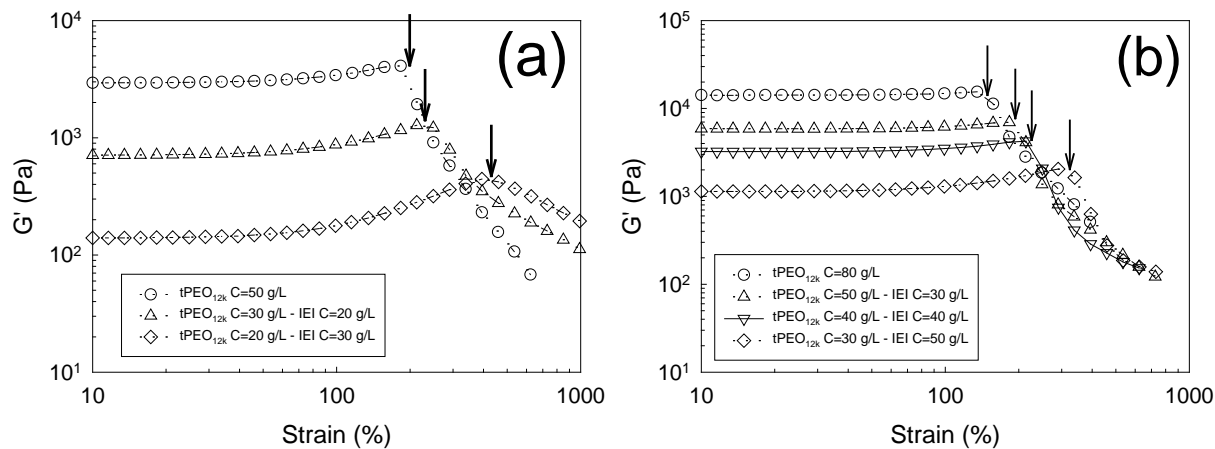
Figure S11. Strain dependence of the elastic modulus (G') for tPEO$_{12k}$/IEI hybrid photo-cross-linked hydrogels at total polymer concentration **(a)** C=50 g/L and **(b)** C=80 g/L and varying the tPEO$_{12k}$/IEI ratio.
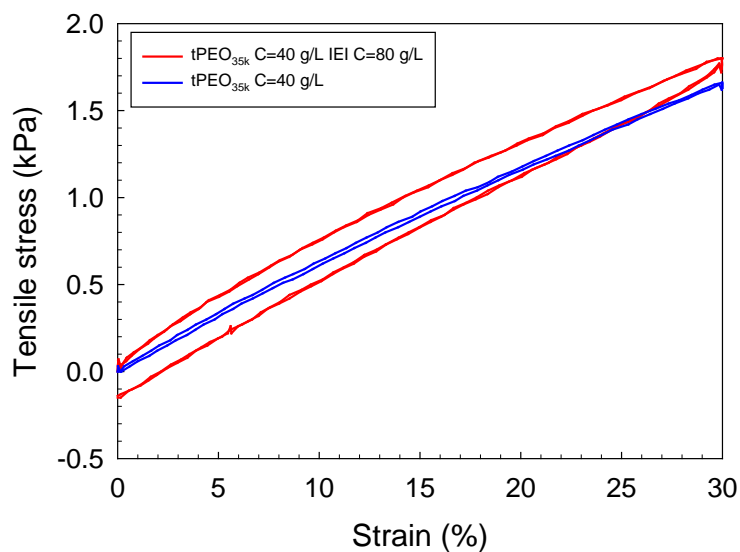

Figure S12. Evolution of the tensile stress with strain during cyclic loading-unloading experiments.

References

(1) Kadam, V. S.; Nicol, E.; Gaillard, C. *Macromolecules* **2012**, *45*, 410-419.

(2) Klymenko, A.; Nicolai, T.; Benyahia, L.; Chassenieux, C.; Colombani, O.; Nicol, E. *Macromolecules* **2014**, *47*, 8386-8393.

(3) Nicol, E.; Derouineau, T.; Puaud, F.; Zaitsev, A. *Journal of Polymer Science Part A: Polymer Chemistry* **2012**, *50*, 3885-3894.

(4) Nicol, E.; Nzé, R.-P. *Macromolecular Chemistry and Physics* **2015**, *216*, 1405-1414.

(5) Piogé, S.; Fontaine, L.; Soutif, J.-C.; Nicol, E.; Pascual, S. *J. Pol. Sci. Part A: Pol. Chem.* **2010**, *48*, 1526-1537.

(6) Kadam, V.; Nicolai, T.; Nicol, E.; Benyahia, L. *Macromolecules* **2011**, *44*, 8225-8232.

(7) Annable, T.; Buscall, R.; Ettelaie, R.; Whittlestone, D. *J. Rheol.* **1993**, *37*, 695-725.

(8) Lauber, L.; Colombani, O.; Nicolai, T.; Chassenieux, C. *Macromolecules* **2016**, *49*, 7469-7477.